Evolution of Inclusions in Fe-13Cr Treated by $CaO-SiO_2-Al_2O_3$-Based Top Slag

QI WANG, LIJUN WANG, JUN ZHAI, JIANMIN LI, and KUO-CHIH CHOU

Experiments were carried out to determine the effect of Al_2O_3 in the slag of the $CaO-SiO_2-Al_2O_3-MgO-CaF_2$ system on the cleanness of Fe-13Cr stainless steel deoxidized by ferrosilicon. Increasing the Al_2O_3 content in basicity = 2.28 slag can reduce the usage of CaF_2 and benefit the obtainment of a good kinetic condition for inclusion removal, but over 21 pct would lead to a higher total oxygen content in the melt and make the inclusion composition more complex. It is found that increasing basicity in 16 pct Al_2O_3 slag would have a good deoxidation ability and accelerate the transformation from high Al_2O_3 inclusions to low melting point $CaO-Al_2O_3-SiO_2-MgO$ system inclusions, but basicity over 2.58 would lead to high content of [Al] in liquid steel, which would promote the formation of $MgO-Al_2O_3$ inclusions. Therefore, it is not suitable to add a high content of Al_2O_3 into high-basicity slag. Adding Al_2O_3 into slag of 2.28 in basicity until a content of 16 pct could achieve inclusion plastication within 45 minutes without Ca treatment, which has potential application in industrial production.

DOI: 10.1007/s11663-016-0852-1

I. INTRODUCTION

RECENTLY, martensitic stainless steels have been widely employed for various usages, including as cutlery materials, due to their high strength, high hardness, and excellent corrosion resistance. The nonmetallic inclusion size distribution, morphology, and chemistry composition have significant effects on its performance. Though inclusions formed unavoidably in the stainless steel, high hardness and high melting point inclusions must be reduced.

Fe-13Cr stainless steels are deoxidized by silicon, due to the harmful effects of Al_2O_3 and $MgO-Al_2O_3$ inclusions on the materials, in the steelmaking process. The ferrosilicon, which is applied in silicon deoxidation, always contains a small amount of aluminum as an impurity.[1] Suzuki[2] calculated Cr13 pct silicon-aluminum complex deoxidation phase stability diagrams and pointed out that $Al_2O_3-SiO_2$ system inclusions could easily form in FeSi-killed stainless steel even when [Al] content is at a quite low level. In fact, $Al_2O_3-SiO_2$ system inclusions are also hard and have a high melting point. However, little attention has been paid to this type of inclusions. Much research has aimed at improving the quality of different steel grades by optimizing the composition of top slag.[3,4] Top slag plays an important role in modifying inclusion chemistry by slag-metal-inclusion reaction and absorbing inclusions in the refining process.[3] Thus, it is important to grasp the influence of top slag on the transformation of $Al_2O_3-SiO_2$ system inclusion in Fe-13Cr stainless steel.

$CaO-SiO_2-CaF_2$-based slag, commonly used in FeSi-killed steel production, has good deoxidation, good desulfurization, and inclusion-removing capacity due to its high basicity.[5,6] However, high-basicity slag generally has a high melting temperature and relatively low fluidity. Thus, CaF_2 will be added to optimize slag properties, but also some negative influences will be presented, such as aggravated refractory erosion and environmental pollution. The contents of CaF_2 and Al_2O_3 in reported top slags are around 15 and 5 pct, respectively.[7–10] Suitable Al_2O_3 content also can lower the melting temperature and reduce CaF_2 usage by Al_2O_3, which would be a good choice. Therefore, in the current study, the $CaO-SiO_2-Al_2O_3$-based slag equilibrium between the Fe-13Cr stainless steel under FeSi(Al) deoxidation was investigated to understand the effect of Al_2O_3 contents and basicity on the composition of $Al_2O_3-SiO_2$ system inclusions.

II. EXPERIMENTS

A. *Materials*

Stainless steel was prepared in a vacuum induction furnace and then cast into ingot under a protecting atmosphere. Table I shows the chemical composition of the stainless steel and top slags used in the experiments. Top slags were prepared by pure CaO, SiO_2, Al_2O_3, MgO, and CaF_2, in which CaO was obtained by calcining $CaCO_3$ (analytical grade) at 1373 K (1100 °C) for 6 hours, and the rest of the oxides were dried at 1273 K (1000 °C) for 4

QI WANG, Ph.D. Student, LIJUN WANG, Associate Professor, and KUO-CHIH CHOU, Professor, are with the State Key Laboratory of Advanced Metallurgy, University of Science and Technology Beijing, and also with the Collaborative Innovation Center of Steel Technology, University of Science and Technology Beijing, 10083, People's Republic of China. Contact e-mail: lijunwang@ustb.edu.cn JUN ZHAI, Researcher, and JIANMIN LI, Senior Researcher, are with the Technical Center, Taiyuan Iron and Steel (Group) Co., Ltd, Taiyuan, Shanxi, 030003, People's Republic of China.

Manuscript submitted June 7, 2016.
Article published online November 30, 2016.

hours in a muffle furnace. The powders were mixed in an agate mortar and then used for the experiments.

B. *Experimental*

In a typical run, an MgO crucible (50-mm i.d., 55-mm o.d., and 115-mm height) containing 400 g of Fe-13Cr stainless steel was placed in a temperature even zone of a vertical $MoSi_2$ resistance furnace. The steel was heated to 1873 K (1600 °C) under high-purity Ar atmosphere; then, in sequence, 0.2 g Fe_2O_3 (to regulate O level to ~150 ppm), 2.5 g FeSi (73 pct Si, 2 pct Al), and 70 g top slag were added. The time when the slag addition completed was defined as the starting time (time zero). Thereafter, steel samples were taken out at 15, 30, 45, 60, and 90 minutes and finally quenched in water.

Each steel sample was cut into three parts. The first part was used for [Al], [Ca], and [Mg] content analysis by inductive coupled plasma atomic absorption spectroscopy (ICP-AAS) or inductive coupled plasma mass spectrometry (ICP-MS). The second part was subjected to total oxygen content (T.O) analysis by using an oxygen/nitrogen determinator (TCH600). The third part of the steel sample was used for microscopic inclusion observation and composition detection by a scanning electron microscope–energy-dispersive spectrometer (FEI Quanta 250), and each sample was observed with 10 view fields under magnification 500 times (0.034 mm^2).

III. RESULTS AND DISCUSSION

As the ferrosilicon used in the present work contained 2 pct aluminum as impurity, the liquid stainless steel was co-deoxidized by Si and Al. Thus, the Al_2O_3-SiO_2-type inclusions were observed in the initial stage with the ratio of Al_2O_3/SiO_2 around 1.5, which also contained trace amounts of CaO, MgO, and MnO. These inclusions mainly exhibited spherical or spheroidic shape.

A. *Physicochemical Properties of CaO-SiO_2-Al_2O_3-MgO-CaF_2 System Slag*

In order to compare the properties of top slag, the melting temperature and viscosity of three Al_2O_3 content levels and three basicity levels were performed by using FactSage6.4 software (Thermfact/CRCT, Canada and GTT-Technologies, Germany). The results are listed in Table II. Here, the properties of top slags are discussed theoretically.

With increasing the amount of Al_2O_3 from 11 to 21 pct, the melting temperature of top slags decreases from 2048 K to 1826 K (1775 °C to 1553 °C) and the percentage of liquid phase increases from 95.37 to 100 pct. From a theoretical viewpoint, Al_2O_3 can effectively reduce the usage of CaF_2. On the contrary, as basicity increases from 1.83 to 2.58, the melting temperature of top slags increases from 1749 K to 1994 K (1476 °C to 1721 °C) and the percentage of liquid phase decreases from 100 to 96.51 pct. Moreover, the viscosity values of the slag at 1873 K (1600 °C) are approximately the same, slightly increasing with Al_2O_3 content and decreasing with basicity.

The activity of CaO, SiO_2, Al_2O_3, and MgO in the top slag were calculated by using FactSage6.4 software (Databases: FToxid, FactPS, FTmisc, and Equilib module), and the results are shown in Table IV. The top slag interacts with liquid steel and further influences the steel chemical composition during the experimental process. The following reactions would occur between the steel and the slag. The steel chemical composition is shown in Table I, and all interaction coefficients are now known from the present work and previous data listed in Table III[11,12] by other researchers:

$$(SiO_2)_{inslag} = [Si] + 2[O] \quad \log K_1 = -24,600/T + 8.4 \text{ [Reference 2]} \quad [1]$$

$$(Al_2O_3)_{inslag} = 2[Al] + 3[O] \quad \log K_2 = -45,300/T + 11.62 \text{ [Reference 13]} \quad [2]$$

$$(CaO)_{inslag} = [Ca] + [O] \quad \log K_3 = -33,714.5/T + 7.62 \text{ [Reference 14]} \quad [3]$$

$$(MgO)_{inslag} = [Mg] + [O] \quad \log K_3 = -4700/T - 4.28 \text{ [Reference 15]} \quad [4]$$

According to Eqs. [1] through [4] and Tables I, III, and IV, the activity of equilibrium-[O] (Eq-a[O]) and the equilibrium contents of [Al] (Eq-[Al]), [Ca] (Eq-[Ca]), and [Mg] (Eq-[Mg]) in liquid steel with top slag can be calculated based on the average content of w[Si] = 0.86 pct, and the results are shown in Table IV. Figure 1 shows the variations of [Si] in test 3, which is used to

Table I. Chemical Composition (Weight Percent) of the Fe-13Cr Stainless Steel and Top Slags

	C	Si	Mn	P	S	Cr	Ni	Al	Ca	Mg
Wt Pct	0.1159	0.557	0.3938	0.0187	0.0019	11.57	0.1195	0.004	0.0005	0.0005

No.	CaO	SiO_2	Al_2O_3	MgO	CaF_2
1	44	24	16	10	5
2	48	21	16	10	5
3	49	19	16	10	5
4	51	22	11	10	5
5	44	19	21	10	5

Table II. Thermophysical Properties of Top Slags

Slag	Number 1 Basicity 1.83 Al_2O_3 16 Pct	Number 2 Basicity 2.28 Al_2O_3 16 Pct	Number 3 Basicity 2.58 Al_2O_3 16 Pct	Number 4 Basicity 2.28 Al_2O_3 11 Pct	Number 5 Basicity 2.28 Al_2O_3 21 Pct
Complete melting point	1749 K (1476 °C)	1929 K (1656 °C)	1994 K (1721 °C)	2048 K (1775 °C)	1826 K (1553 °C)
Liquid slag percentage at 1873 K (1600 °C)	100 pct	98.95 pct	96.51 pct	95.37 pct	100 pct
Slag viscosities (Pa s) at 1873 K (1600 °C)	0.084	0.073	0.068	0.065	0.081

Table III. Interaction Coefficient Employed in This Study[11,12]

j	Al	Si	Cr	C	Ni	O	Mn	S
e_{Si}^{j}	0.058	0.103	−0.021	0.18	−0.009	−0.119	0.0042	0.066
e_{Al}^{j}	0.043	0.056	0.012	0.091	−0.029	−1.98	0.035	0.035
e_{Mg}^{j}	−0.12	−0.088	0.047	−0.31	−0.012	−460	—	—
e_{Ca}^{j}	−0.072	−0.097	0.02	−0.34	−0.044	−5600[12]	−0.007	−140

characterize the variation of [Si] in all tests. Because of the significant quantitative differences between [Si] and the content of other elements, [Si] could be considered to have few changes after direct deoxidation.

As shown in Table IV, a[O], Eq-[Al], Eq-[Ca], and Eq-[Mg] increased with Al_2O_3 content in the top slag. Table IV also indicates that Eq-[Al], Eq-[Ca], and Eq-[Mg] increased while a[O] decreased with the increase of slag basicity and a[O] decreased with the increase of slag basicity.

B. *Effect of Alumina in Slag*

1. *Evolution of steel chemical composition during slag-steel reaction*

The variations of steel chemical compositions are shown in Figure 2. As for the [Al] content, in Figure 2(a), it mainly increased with reaction time. The content in test 5 reached 60 to 90 ppm, higher than the other tests, which indicated that the content of [Al] in stainless steel is proportional to the Al_2O_3 content in slag. The [Ca] content variation is shown in Figure 2(b). The [Ca] content varied within the range of 5 to 15 ppm during the reaction process in all three tests and slightly increased with the increase of Al_2O_3 content in slag. In the case of [Mg], it was generally much lower than the content of [Ca]. Figure 2(c) shows that the content of [Mg] is lower at the initial reaction process in test 5 (basicity 2.28, Al_2O_3 21 pct) and has a stable content in the other tests. In Figure 2(d), the value of TO in steel decreased with the increase of Al_2O_3 content first and then increased with the increase of Al_2O_3 content at the same basicity. It can be obtained, by comparing the element contents of Ca and Al calculated with those measured, that they could be transferred into liquid steel, while Mg is hard to transfer into liquid steel. This result also can be taken as evidence for 21 pct Al_2O_3 in top slag leading to lower [Mg] content, which might be related to the formation of MgO-Al_2O_3 system inclusions.

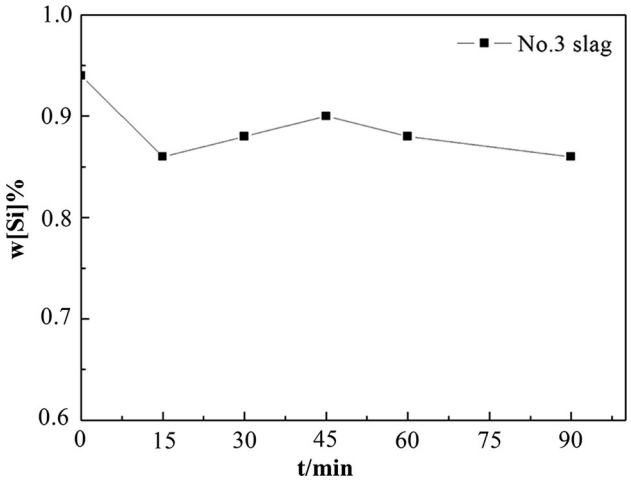

Fig. 1—Variation of [Si] in test 3.

2. *Evolution of inclusions during the slag-steel reaction*

The effects of alumina in top slags on the average size and inclusion area fraction of the stainless steel are demonstrated in Figure 3. The average sizes of the inclusions in the three tests were around 2 μm and did not change considerably during the reaction process. Figure 3(b) shows that the inclusion area fractions decreased with the increase of reaction time in the three tests, indicating that inclusion flotation and absorption occurred in all types of top slag. Moreover, the highest inclusion area fractions were observed in the final steel samples of test 5 (basicity 2.28, Al_2O_3 21 pct), which implies that excessive high content of Al_2O_3 in slag may hinder the capacity of absorbing inclusions.

Figure 4 shows the effect of alumina in top slags on the variations of typical inclusions with reaction time. Figure 4(a) shows the composition distribution of inclusions at different reaction times, and Figure 4(b) shows the morphology and main composition of typical inclusions. The inclusion evolution process had four steps. (1) The Al_2O_3-SiO_2 system inclusions were generated after FeSi(Al) alloy was added into liquid steel.

Table IV. Activity of CaO, SiO_2, Al_2O_3, and MgO in Top Slags and the Equilibrium Content of [Al], [Ca], and [Mg], and Activity of [O], in Liquid Steel at 1873 K (1600 °C)

	Top Slag				Molten Steel			
No.	a_{Al2O3}	a_{SiO2}	a_{CaO}	a_{MgO}	a[O]	$[Al]_{eq}$	$[Ca]_{eq}$	$[Mg]_{eq}$
1	8.01×10^{-3}	9.30×10^{-4}	3.58×10^{-2}	1.11×10^{-1}	1.6×10^{-4}	0.0137 pct	0.0029 pct	0.0001 pct
2	3.25×10^{-3}	2.91×10^{-4}	6.77×10^{-2}	1.49×10^{-1}	9×10^{-5}	0.0209 pct	0.0098 pct	0.00028 pct
3	2.08×10^{-3}	1.70×10^{-4}	9.0×10^{-2}	1.49×10^{-1}	7×10^{-5}	0.025 pct	0.0170 pct	0.00036 pct
4	9.49×10^{-4}	1.45×10^{-4}	1.08×10^{-1}	1.49×10^{-1}	6.9×10^{-5}	0.019 pct	0.0223 pct	0.00039 pct
5	7.34×10^{-3}	4.67×10^{-4}	4.73×10^{-2}	1.32×10^{-1}	1.2×10^{-4}	0.022 pct	0.0054 pct	0.00019 pct

(2) The content of Al_2O_3 in inclusions increased after top slag was added into the liquid steel. (3) High-Al_2O_3 inclusions were transformed to low melting temperature CaO-SiO_2-Al_2O_3-MgO inclusions or $MgAl_2O_4$ inclusions wrapped with CaO-SiO_2-Al_2O_3-MgO inclusions with reaction time, depending on the amount of Al_2O_3 in the slag phase. (4) The content of MgO increased with reaction time in these two kinds of inclusions and would change to high MgO complex inclusions, even pure MgO inclusions, at 90 minutes.

From the experimental result, adding 16 pct content of Al_2O_3 in the 2.28 basicity slag would reduce the usage of CaF_2, not lead to MgO-Al_2O_3 inclusion formation in stainless steel, and have a good capacity for absorbing inclusions. Therefore, the addition of Al_2O_3 in slag has a limitation, especially in high-basicity slag.

C. *Effect of Slag Basicity*

1. *Evolution of steel chemical composition during slag-steel reaction*

The variations of steel chemical compositions are shown in Figure 5. According to Figure 5(a), [Al] contents in test 3 (basicity 2.58, Al_2O_3 16 pct) are higher than the other tests. This finding indicates that increasing slag basicity would decrease the activity of Al_2O_3 in slag and the activity of [O] in steel, as shown in Table IV, which would increase the content of [Al] in steel. As shown in Figure 5(b), [Ca] contents varied within the range of 0.0005 to 0.0015 pct during the reaction process in all three basicity levels and slightly increased with the increase of slag basicity. Figure 5(c) shows that the steel content of [Mg] has lower contents at the front of the reaction process in test 3 (basicity 2.58, Al_2O_3 16 pct) and has a stable content of [Mg] in the other tests. Excessive high-basicity slag may lead to a lower [Mg] content, as in test 5 (basicity 2.28, 21 pct Al_2O_3), which might be related to the formation of MgO-Al_2O_3 system inclusions. As seen in Figure 5(d), the value of TO in steel decreases with the increase of basicity, but when the slag basicity is over about 2.28, the total oxygen content tends to be stable.

2. *Evolution of inclusions during the slag-steel reaction*

The effects of slag basicity on the average size and inclusion area fractions of the stainless steel are demonstrated in Figure 6. The average inclusion sizes in the three basicity levels were around 2 μm, and the inclusion area fraction decreased with the increase of reaction time, similar to the Al_2O_3 content change slags. Moreover, the lowest inclusion area fraction was observed in the final steel samples of test 2 (basicity 2.28, Al_2O_3 16 pct), which implied that appropriate high basicity in slag might enhance the capacity of absorbing inclusions.

Figure 7 shows the effect of slag basicity change on the variations of typical inclusions with reaction time. The evolution process is similar to that in the series of Al_2O_3 effects; *i.e.*, it started from SiO_2-Al_2O_3 system inclusions, next high-Al_2O_3 inclusions, then CaO-SiO_2-Al_2O_3-MgO inclusions, and finally part of CaO-SiO_2-Al_2O_3-MgO inclusions, which transformed to high-MgO inclusions. An exception was that MgO-Al_2O_3 inclusions appeared in all the steel samples when the top slag basicity was 2.58. It can also be obtained from Figure 6 that inclusions in test 2 (basicity 2.28, Al_2O_3 16 pct) could achieve plasticization within 45 minutes, which is significant for industrial production.

D. *Thermodynamic Calculation on Evolution of Inclusions*

Thermodynamic calculations were carried out to evaluate the evolution of inclusions in Fe-13Cr stainless steel. Two stability diagrams of Ca-Al (0.0008 pct Mg) and Mg-Al (0.0008 pct Ca) were calculated using FactSage6.4 software (Databases: FToxid, FactPS, FTmisc, and Phase Diagram module) based on the Fe-13Cr stainless steel chemical composition at 1873 K (1600 °C). The results are shown in Figure 8.

Figure 8(a) shows the Slag-liq phase at 1873 K (1600 °C), along with points corresponding to the experimental [Ca] and [Al] contents in the final sample (90 minutes). As can be seen, three data points located in the Slag-liq phase, while excessive basicity resulted in spinel formation, consistent with the experimental observation. A comparison of the measured contents ([Mg] and [Al] in a 90-minute sample) with the calculated stability diagram is given in Figure 8(b). As seen in Figure 8(b), almost all data points are located in the Slag-liq phase, while excessive Al_2O_3 content resulted in spinel formation, which further indicates that the formation of MgO-Al_2O_3 could be easier with the increase of [Al] in Fe-13Cr stainless steel.

E. *Kinetic Calculation on Evolution of Inclusions*

Generally, the inclusion modification process should include two microprocesses: (1) the mass-transfer

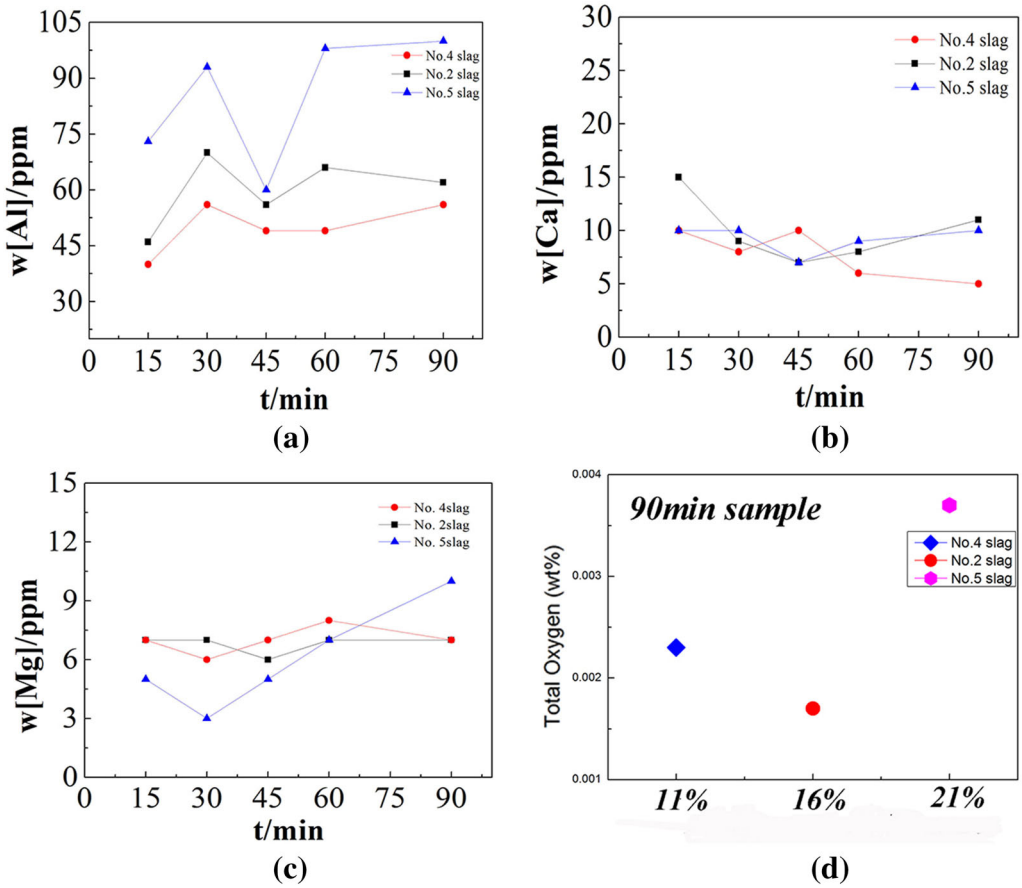

Fig. 2—Variation of steel composition (*a*) [Al], (*b*) [Ca], (*c*) [Mg], and (*d*) T.O in the series tests with different Al_2O_3 content in slag.

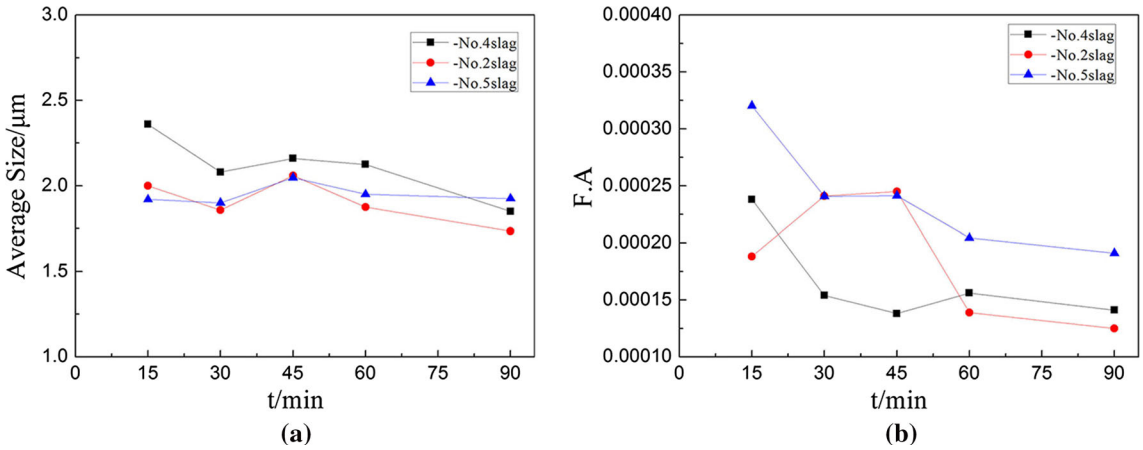

Fig. 3—Variations of (*a*) average inclusion size and (*b*) area fraction in the series of tests with different Al_2O_3 content in slag.

process between slag and molten steel and (2) the inclusion modification process between inclusion and molten steel. Figure 9 shows these two microprocesses in schematic form.

Okuyama[16] established a slag-steel-inclusions model based on the two-film theory and the unreacted core model to investigate the effect of slag composition on the kinetics of formation of $MgO\text{-}Al_2O_3$ inclusions. This slag-steel-inclusions model is also appropriate for our experiments. He concludes that, in the system as a whole, the slag-steel reaction is the rate-determining step for the rate of inclusion formation.

In the case of the first microprocesses, a kinetic study was carried out based on a two-film theory to figure out the rate-determining step in this process, using slag 2 as an example. The results are listed in Table V. The mass transfer of [Al] and [Ca] in molten steel was the rate-determining step, which agreed with former studies.[17,18] When compared, the maximum diffusion rates of [Ca] in the experiment are far less than those of [Al].

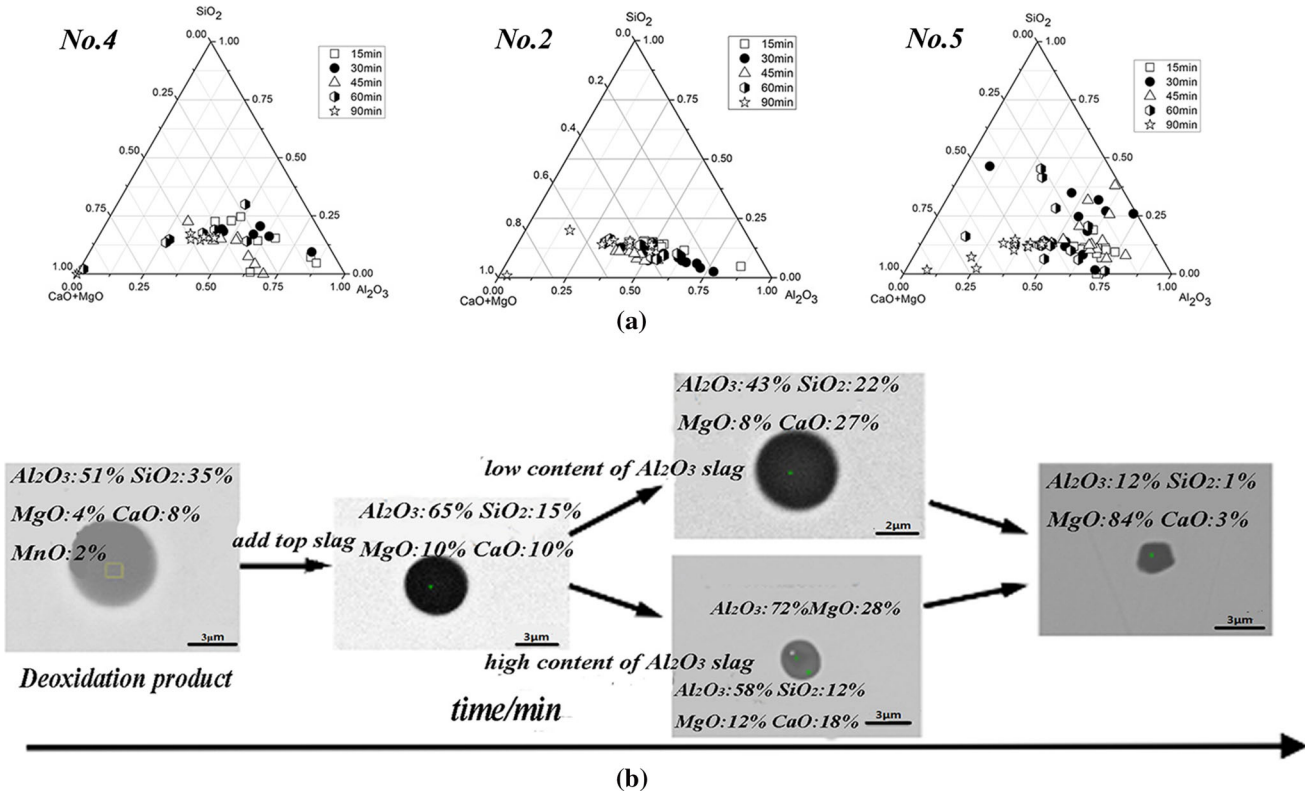

Fig. 4—Evolution process of inclusions in the series of tests with different Al_2O_3 content in slag (*a*) inclusion composition variations plotted in CaO-SiO_2-Al_2O_3 phase diagram; (*b*) SEM photos of typical inclusions.

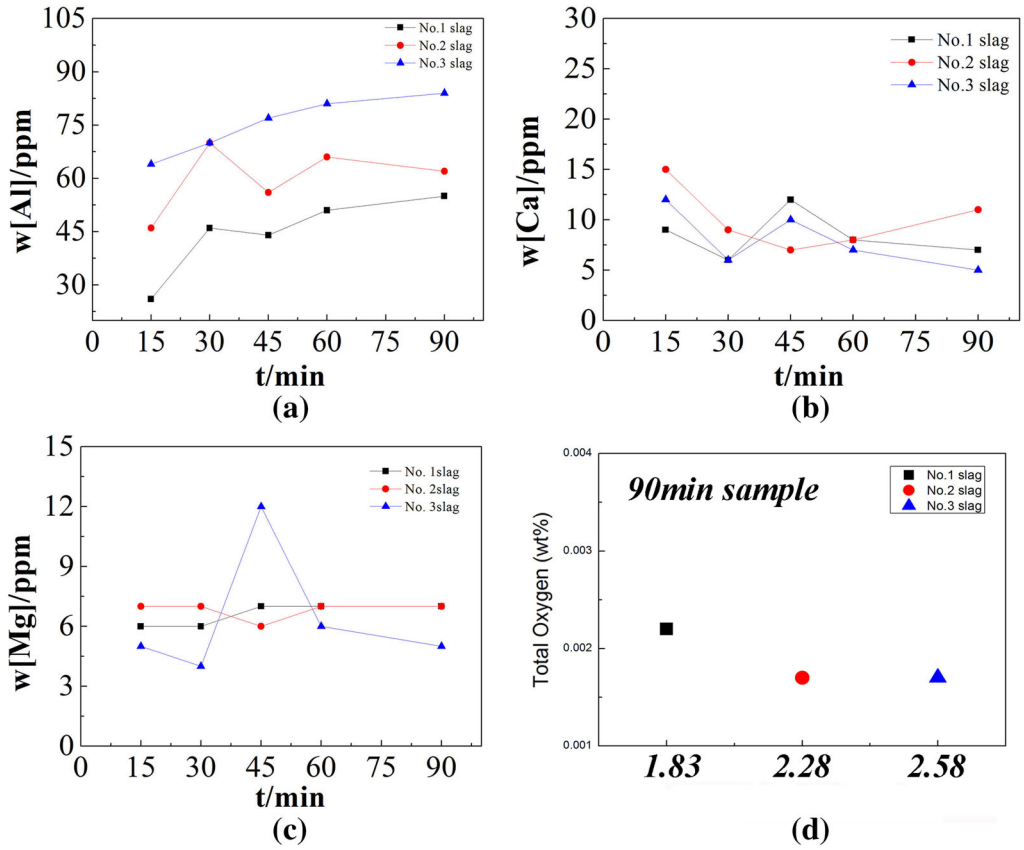

Fig. 5—Variation of steel composition (*a*) [Al], (*b*) [Ca], (*c*) [Mg], and (*d*) T.O in the series of tests with different basicity in slag.

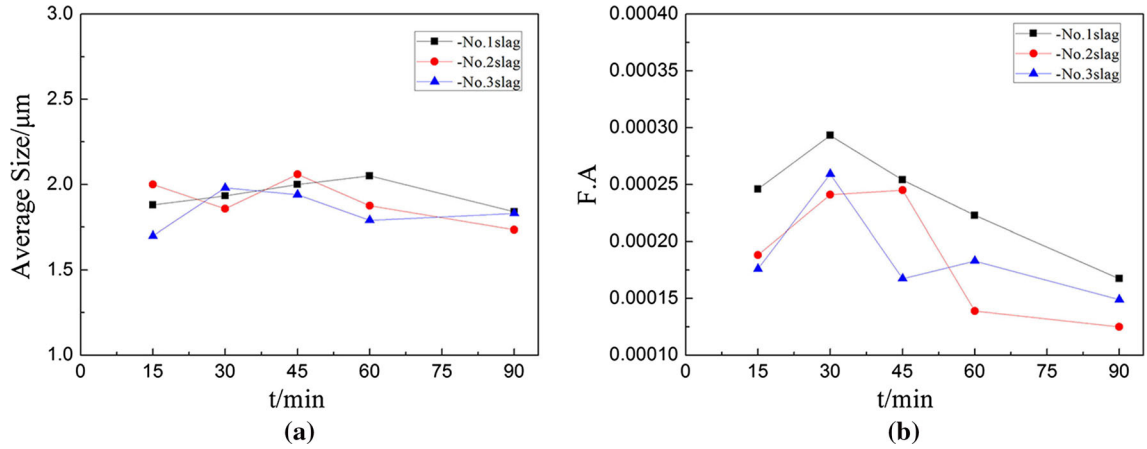

Fig. 6—Variations of (*a*) average inclusion size and (*b*) area fraction in the series of tests with different basicity in slag.

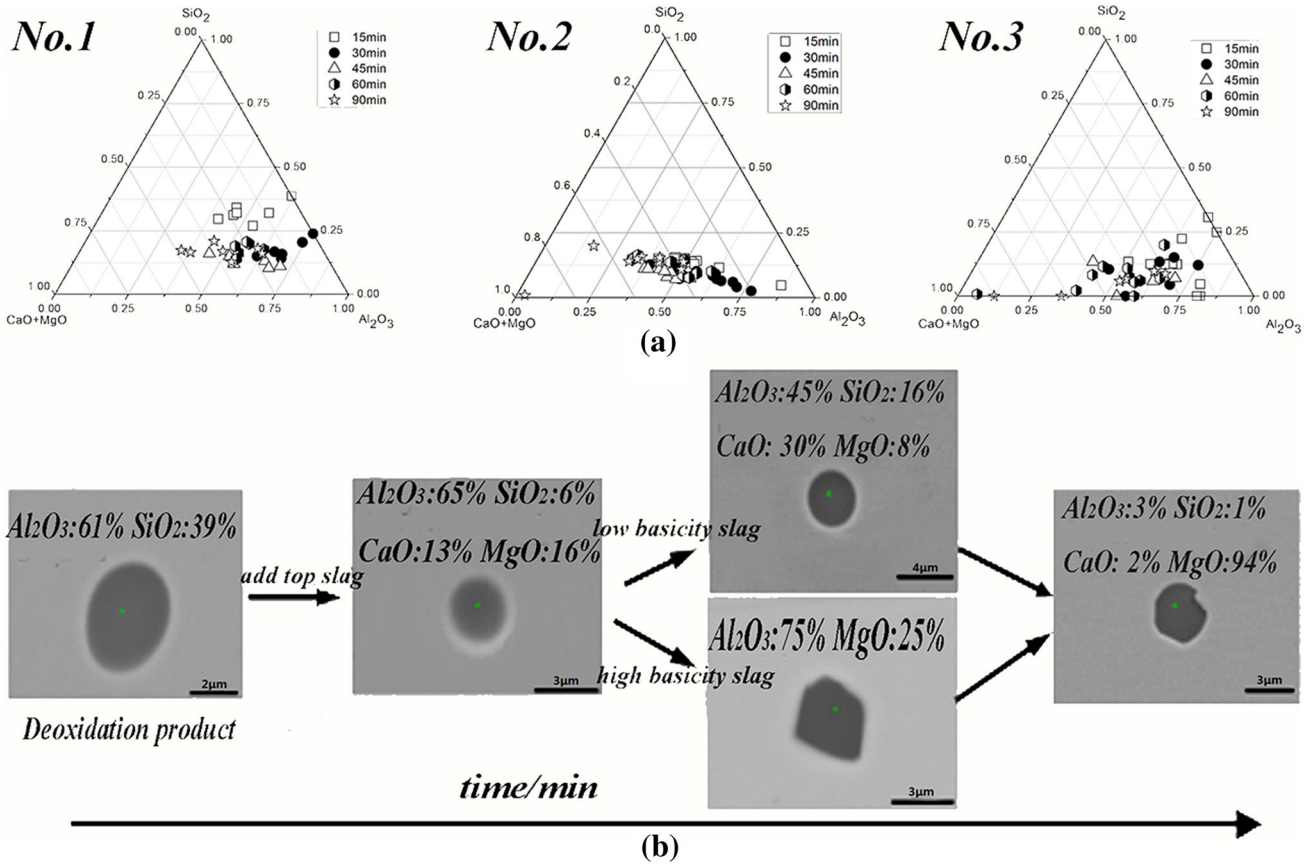

Fig. 7—Evolution process of inclusions in the series of tests with different basicity in slag (*a*) inclusion composition variations plotted in CaO-SiO_2-Al_2O_3 phase diagram; (*b*) SEM photos of typical inclusions.

Table V. Calculated Maximum Diffusion Rate for Metal Transfer in Steel Side for Experiment 2

$n_{[Al]}$/mol s^{-1}	$n_{[Ca]}$/mol s^{-1}
3.78×10^{-6}	4.45×10^{-7}

Therefore, it was considered that the [Ca] mass transport in the steel side would be the possible rate-controlling step during the reaction process. The result showed good agreement with our experimental results.

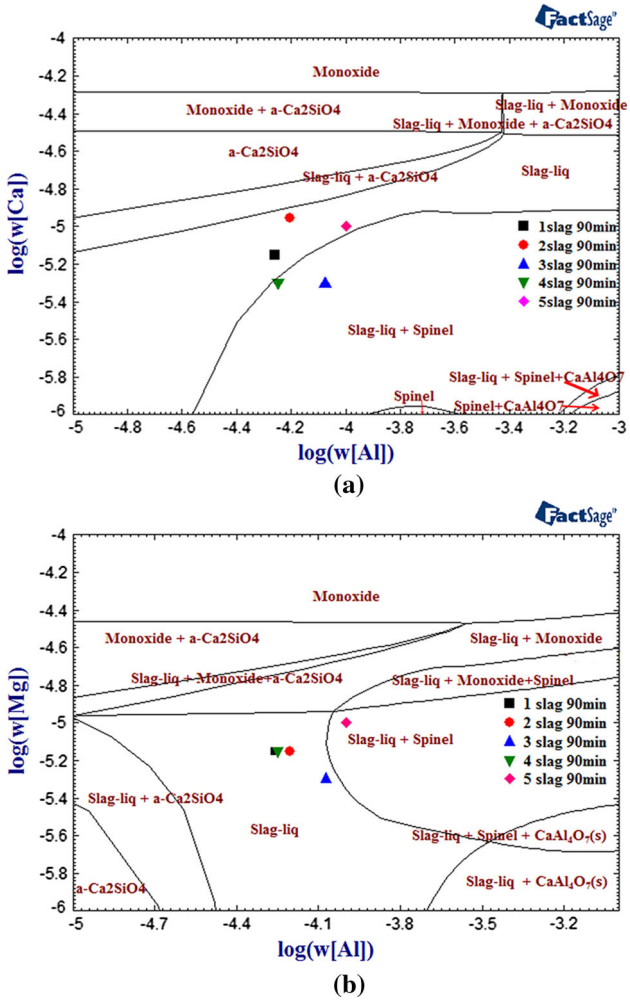

Fig. 8—Stability diagrams of (*a*) Ca-Al-O (0.0008 pct Mg) and (*b*) Mg-Al-O (0.0008 pct Ca) in Fe-13Cr stainless steels at 1873 K (1600 °C).

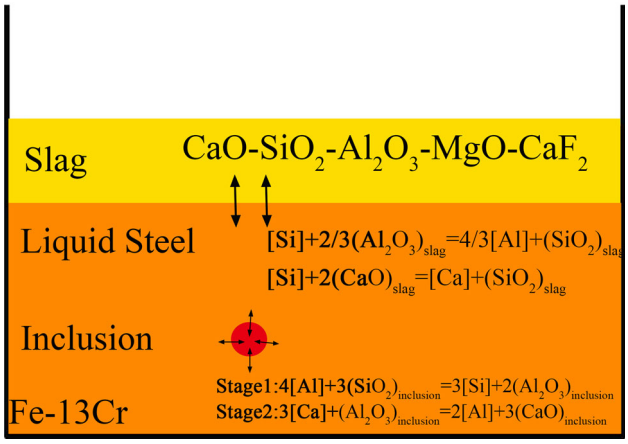

Fig. 9—Schematic diagram for the reactions of slag with liquid steel and liquid steel with inclusions.

IV. CONCLUSIONS

Ladle treatment of Fe-13Cr stainless steel was simulated on a laboratory scale. The effects of slag chemistry on the steel and inclusion compositions were discussed with thermodynamic and kinetics considerations. The steel cleanliness in terms of factors for different types of slags is compared. The main results are as follows.

1. In FeSi(Al) alloy–killed stainless steel, Al_2O_3-SiO_2 system inclusion formed initially, as expected, and then changed to CaO-Al_2O_3-SiO_2-MgO complex inclusions characteristic of high Al_2O_3 composition, near the Al_2O_3 corner in the Ca(Mg)O-SiO_2-Al_2O_3 diagram. The modification role of the top slag on inclusions gave the inclusion composition a relatively lower melting point region as time went on. A proper reaction time is necessary to obtain low melting point inclusions, but too long of a reaction time would lead to the generation of high-MgO inclusion.
2. At the same basicity level, CaO-MgO-Al_2O_3-SiO_2 system inclusions were achieved instead of spinel inclusions with increasing Al_2O_3 content in the top slag. However, when the Al_2O_3 content reached 21 pct or higher, a complex inclusion as the Mg-Al-O system was wrapped by CaO-MgO-Al_2O_3-SiO_2 inclusion was generated. Moreover, 21 pct Al_2O_3 also increases the total oxygen content in stainless steel and has a negative effect on absorb inclusions. Therefore, the addition of Al_2O_3 in slag has limitations, especially in high-basicity slag.
3. At the same Al_2O_3 content level, an increase in slag basicity could accelerate the transition from high Al_2O_3 inclusions to low melting point CaO-Al_2O_3-SiO_2-MgO system inclusions. However, excessive high basicity (over 2.58) would cause high content of [Al] in liquid steel, which would promote the MgO-Al_2O_3 formation.
4. Adding 16 pct content of Al_2O_3 in 2.28 basicity slag could achieve inclusion plastication within 45 minutes without Ca treatment and reduce the usage of CaF_2, which has potential application in industrial production. In this condition, the addition of Al_2O_3 in slag did not lead to MgO-Al_2O_3 inclusion formation in stainless steel.

ACKNOWLEDGMENTS

The authors express their appreciation to the National Nature Science Foundation of China (Grant Nos. 51104013, 51174022, and 51374020), the Fundamental Research Funds for the Central Universities (Grant No. FRF-TP-15-052A3), the Beijing Higher Education Young Elite Teacher Project (Grant No. YETP0349), and the China Postdoctoral Science Foundation (Grant No. 2014M560046).

REFERENCES

1. T Fujisawa, M Suzuki, Y Wanibe, and H Sakao: *Tetsu-to-Hagané*, 1986, vol. 72, pp. 218–24.
2. K Suzuki, S Banya, and M Hino: *ISIJ Int*., 2001, vol. 41, pp. 813–17.
3. P Yan, S Huang, L Pandelaers, J Vandyck, M Guo, and B Blanpain: *Metall. Mater. Trans. B*, 2013, vol. 44B, pp. 1105–19.
4. W Yang, X Wang, L Zhang, Q Shan, and X Liu: *Steel Res. Int*., 2013, vol. 84, pp. 473–89.
5. H Suito and R Inoue: *ISIJ Int*., 1996, vol. 36, pp. 528–36.
6. PK Iwamasa and RJ Fruehan: *Metall. Mater. Trans. B*, 1997, vol. 28B, pp. 47–57.
7. K Mizuno, H Todoroki, M Noda, and T Tohge: *Iron Steelmaker*, 2001, vol. 28, pp. 93–101.
8. JW Kim, SK Kim, DS Kim, YD Lee, and PK Yang: *ISIJ Int*., 1996, vol. 36, pp. S140–S143.
9. K Sakata: *ISIJ Int*., 2006, vol. 46, pp. 1795–99.
10. Y Ehara, S Yokoyama, and M Kawakami: *Tetsu-to-Hagané*, 2007, vol. 93, pp. 475–82.
11. Steelmaking Data Sourcebook: *The Japan Society for the Promotion of Science, The 19th Committee on Steelmaking*, Goldon Breach Science, New York, 1988.
12. MP Howard and B Debanshu: *Metall. Mater. Trans. B*, 1984, vol. 15B, pp. 547–62.
13. H Itoh and M Hino: *Metall. Mater. Trans. B*, 1997, vol. 28B, pp. 953–56.
14. H Ohta and H Suito: *ISIJ Int*., 2003, vol. 43, pp. 1293–1300.
15. MH Zayan, OM Jamjoom, and NA Razik: *Oxide Metall*., 1990, vol. 34, pp. 323–33.
16. G Okuyama, K Yamaguchi, S Takeuchi, and K Sorimachi: *ISIJ Int*., 2000, vol. 40, pp. 121–28.
17. D Kim and JH Park: *Metall. Mater. Trans. B*, 2012, vol. 43B, pp. 875–86.
18. JH Park: *Metall. Mater. Trans. B*, 2007, vol. 38B, pp. 657–63.